Published in final edited form as:
J Cogn Neurosci. 2013 June ; 25(6): 862–871. doi:10.1162/jocn_a_00370.

Spatial Frequency Tuning Reveals Interactions between the Dorsal and Ventral Visual Systems

Bradford Z. Mahon[1], **Nicholas Kumar**[1], and **Jorge Almeida**[2,3,4]

[1]University of Rochester

[2]University of Coimbra

[3]University of Minho

[4]University of Lisbon

Abstract

It is widely argued that the ability to recognize and identify manipulable objects depends on the retrieval and simulation of action-based information associated with using those objects. Evidence for that view comes from fMRI studies that have reported differential BOLD contrast in dorsal visual stream regions when participants view manipulable objects compared with a range of baseline categories. An alternative interpretation is that processes internal to the ventral visual pathway are sufficient to support the visual identification of manipulable objects and that the retrieval of object-associated use information is contingent on analysis of the visual input by the ventral stream. Here, we sought to distinguish these two perspectives by exploiting the fact that the dorsal stream is largely driven by magnocellular input, which is biased toward low spatial frequency visual information. Thus, any tool-selective responses in parietal cortex that are driven by high spatial frequencies would be indicative of inputs from the ventral visual pathway. Participants viewed images of tools and animals containing only low, or only high, spatial frequencies during fMRI. We find an internal parcellation of left parietal "tool-preferring" voxels: Inferior aspects of left parietal cortex are driven by high spatial frequency information and have privileged connectivity with ventral stream regions that show similar category preferences, whereas superior regions are driven by low spatial frequency information. Our findings suggest that the automatic activation of complex object-associated manipulation knowledge is contingent on analysis of the visual input by the ventral visual pathway.

INTRODUCTION

A basic distinction within primate vision is between a dorsal visual object-processing stream that projects from primary visual cortex to posterior parietal cortex and a ventral visual object-processing stream that projects from primary visual cortex to ventral temporal cortex (Goodale & Milner, 1992; Felleman & Van Essen, 1991; Ungerleider & Mishkin, 1982). The classic understanding of the dorsal visual system is that it computes spatial and volumetric properties from the visual input to support grasping, locomotion, and eye movements, whereas ventral pathways extract object identity across variation in orientation, distance, and size. Lesions to dorsal stream regions can lead to visuomotor impairments leaving object identification unaffected, whereas ventral stream lesions can impair object

Reprint requests should be sent to: Bradford Z. Mahon, Meliora Hall, University of Rochester, Rochester, NY 14627-0268, or via mahon@rcbi.rochester.edu.

identification while sparing visuomotor abilities (Pisella, Binkofski, Lasek, Toni, & Rossetti, 2006; Goodale & Milner, 1992).

One difference between the types of visual information that are processed within the ventral and dorsal streams originates in two types of retinal ganglion cells. Midget ganglion cells are sensitive to middle-to-high spatial frequencies (HSF) and project information through parvocellular nerve pathways, whereas parasol ganglion cells are sensitive to low spatial frequencies (LSF) and relay information through magnocellular nerve pathways (Livingstone & Hubel, 1988; Tootell, Silverman, Hamilton, Switkes, & De Valois, 1988; Derrington & Lennie, 1984). Although parvocellular and magnocellular information mixes already in V1 (Merigan & Maunsell, 1993; Maunsell, Nealey, & DePriest, 1990; Livingstone & Hubel, 1988), there is an asymmetry in the way the two channels of information are passed on to the ventral and dorsal streams (Merigan & Maunsell, 1993): The ventral visual pathway receives both magnocellular and parvocellular inputs (Ferrera, Nealey, & Maunsell, 1992), whereas the dorsal visual pathway receives largely magnocellular input (Merigan & Maunsell, 1993).

It is known that viewing manipulable objects such as tools and utensils leads to differential BOLD contrast in posterior parietal regions (Mahon et al., 2007; Noppeney, Price, Penny, & Friston, 2006; Chao & Martin, 2000). Despite Goodale and Milner's alignment of the dorsal visual pathway hypothesis with the superior parietal lobule (e.g., Milner & Goodale, 1995; Goodale & Milner, 1992), differential BOLD contrast in both inferior and superior parietal cortex for manipulable objects has been widely regarded as monolithically deriving from an analysis of the visual input by the dorsal object processing stream. An important theory based on that supposition, the Embodied Cognition Hypothesis of tool recognition, argues that visual recognition of manipulable objects depends on simulation of motor-based information (e.g., Noppeney et al., 2006; Gallese & Lakoff, 2005; Martin, Ungerleider, & Haxby, 2000; for discussion, see Kiefer & Pulvermüller, 2012). That theory is thus committed to the view that motor information is retrieved independently of analysis of the visual input by ventral stream structures. It should be noted that many positive claims about the embodiment of tool concepts are not construed as claims about object identification per se (e.g., see Buccino et al., 2005; Gallese & Lakoff, 2005; Barsalou, 1999; for overview, see Kiefer & Pulvermüller, 2012); however, they are nevertheless committed to specific hypotheses about the processes involved in object identification. This is because those arguments about the embodiment of tool concepts take the form: (i) Motor knowledge is constitutive, at least in part, of object concepts; thus, (ii) manipulable object concept retrieval includes motor retrieval (hence the observation is explained that the motor system is activated during conceptual processing of manipulable objects). If the assumption is accepted that concept retrieval is a necessary step in object identification (the denial of which would seem untenable), then it follows that, on such accounts, object identification entails motor retrieval.

The logic of the current investigation is to use spatial frequencies to gain leverage on the critical issue of whether the retrieval of object-associated manipulation knowledge is contingent on analysis of the visual input by the ventral object processing stream. As noted above, there is a strong bias against HSF information being processed by the dorsal object processing stream. Thus, in the measure to which tool preferences are observed in parietal cortex for stimuli containing only HSF, then it follows that those object representations are contingent on analysis of the visual input by ventral visual structures. If that were the case, then the core assumption of the embodied cognition framework as it applies to manipulable object identification would be undermined, and a theory of object recognition would have to explore how activation of some motor-relevant information about objects is contingent on ventral stream processes.

METHODS

Participants

Forty participants were tested (mean age = 20.1 years, *SD* = 1.2 years). Twenty-five participants completed Experiment 1, and 15 participants completed Experiment 2. All participants had normal or corrected-to-normal eyesight and no history of neurological disorders. All guidelines and requirements of the University of Rochester's Research Subjects Review Board were followed for participant recruitment and experimental procedures.

Experimental Stimuli

Stimuli were black-and-white pictures of animals and tools on a gray background. Thirty-two animal and 32 tool objects were used, with two exemplars for each object (total of 128 pictures). The words corresponding to the tool and animal names were matched on length in letters (means, standard deviations in parenthesis: animals = 5.5 (2.0), tools = 5.9 (2.4); $t < 1$), lexical frequency using the CELEX database (animals = 22.8 (30.6), tools = 20.2 (37.2); $t < 1$), and concept familiarity using the MRC Online Psycholinguistic Database (animals = 519.8 (33.9), tools = 519.3 (62.4); $t < 1$). The pictures were enclosed in a 200 × 200 square pixel frame and subtended ~4° of visual angle (viewing angle: ~47 pixels per degree). The spatial frequency content of the original broadband images was filtered to create HSF and LSF filtered versions of the pictures using Matlab (Matlab 2009). Briefly, images were Fourier transformed into frequency space, the target frequencies were filtered, and the filtered images were transformed back to their original space through an inverse Fourier transform. To create HSF items, we used a highpass cutoff that was higher than seven cycles per degree, and to create the LSF items, we filtered the pictures using a low-pass cutoff that was lower than one cycle per degree. Average luminance of the pictures did not differ between the three spatial frequency conditions (broadband, HSF, LSF; mean luminance across all stimuli was 132.62, 132.60, and 132.62 on a 255 grayscale for broadband, HSF, and LSF images, respectively; $F(2, 381) < 1$). Moreover, average luminance within each spatial frequency condition did not differ between the two semantic categories (broadband images: 131.60 and 133.64 for animal and tools, respectively, $t(63) = 1.5$, $p = .135$; HSF images: 131.59 and 133.63 for animal and tools, respectively, $t(63) = 1.5$, $p = .133$; LSF images: 131.60 and 133.65 for animal and tools, respectively, $t(63) = 1.515$, $p = .135$).

General Procedure

"A simple framework" (Schwarzbach, 2011) was used to control stimulus presentation and response collection in Psych toolbox in MATLAB on a MacPro running Windows (Brainard, 1997; Pelli, 1997). Stimuli were back projected (temporal resolution = 120 Hz) on a screen that participants viewed with a mirror attached to the head coil.

Experiment 1

Participants viewed the tool and animal stimuli passively (no response) in a miniblock design. Within each 16-sec miniblock, 32 animals or 32 tools were presented (duration= 500 msec, ISI = 0). Miniblocks of stimuli were separated by 16 sec of fixation. Each exemplar ($n = 2$) was presented twice per run resulting in four miniblocks of animals and four miniblocks of tools for each run. Baseline conditions consisted of scrambled versions of the same stimuli, creating "scrambled animal" and "scrambled tool" conditions that preserved (but randomly displaced) local low-level visual information (scrambling kernel = 32 pixels). All participants completed two runs of the protocol in Experiment 1 (each run lasted ~9 min).

Experiment 2

Experiment 2 followed the same design and procedure as Experiment 1 except for the inclusion of two additional conditions: HSF and LSF images of tools and animals, both intact and scrambled. As in Experiment 1, each run contained a balanced experimental design (each run lasted ~7.5 min). Participants completed between five and eight runs.

MRI Parameters

Whole-brain BOLD imaging was conducted on a 3T Siemens MAGNETOM Trio scanner with a 32-channel head coil at the Rochester Center for Brain Imaging. High-resolution structural T1 contrast images were acquired using a magnetization prepared rapid gradientecho pulse sequence at the start of each session (repetition time = 2530 msec, echo time = 3.44 msec, flip angle = 7°, field of view = 256 mm, matrix = 256 × 256, 1 × 1 × 1 mm sagittal left-to-right slices). An EPI pulse sequence was used for T2* contrast (repetition time= 2000 msec, echo time= 30 msec, flip angle = 90°, field of view = 256 mm, matrix 64 × 64, 30 sagittal left-to-right slices, voxel size = 4 × 4 × 4 mm). The first six volumes of each run were discarded to allow for signal equilibration.

fMRI Data Analysis

fMRI data were analyzed with the Brain Voyager software package (Version 2.1) and in-house scripts drawing on the BVQX toolbox for MATLAB. Preprocessing of the functional data included, in the following order, slice time correction (sinc interpolation), motion correction with respect to the first volume of the first functional run, and linear trend removal in the temporal domain (cutoff: two cycles within the run). Functional data were registered (after contrast inversion of the first volume) to high-resolution deskulled anatomy on a participant-by-participant basis in native space. For each participant, echo-planar and anatomical volumes were transformed into standardized (Talairach & Tournoux, 1988) space. Functional data were smoothed at 6-mm (1.5 voxels) FWHM and interpolated to 3 × 3 × 3 mm voxels.

The general linear model was used to fit beta estimates to the events of interest. The first derivatives of 3-D motion correction from each run were added to all models as regressors of no interest to attract variance attributable to head movement. All analyses treated participants as a random factor, and there were thus 24 and 14 *df* in the group-level analyses in Experiments 1 and 2, respectively. Experimental events were convolved with a standard two gamma hemodynamic response function. In Experiment 1, there were six regressors: the 2 × 2 design of the first/second presentation of images (factor not analyzed herein) and the category of the stimulus (tools and animals) as well as the scrambled versions of tools and animals. In Experiment 2, there were 12 predictors of interest, corresponding to the orthogonal crossing of the following three factors: spatial frequency (HSF, LSF, broadband), category (tool, animal), and image type (intact, scrambled).

All functional connectivity analyses were time-course-based and used the time series from the entire run. Time courses were extracted from preprocessed functional data that had also been regressed with the outputs from motion correction (change in head position across volumes) and the global mean time course from the whole brain. All connectivity was then computed over the residuals from that model. Whole-brain functional connectivity maps were computed with a mask fit to the deskulled talairached anatomy. Whole-brain maps were computed on a run-by-run basis, and the run-specific *r* maps were then averaged (within voxel) for each participant. Group-level statistics were computed using a one-sample *t* test against zero within each voxel across participants.

RESULTS

Inferior-to-superior Organization by Spatial Frequency within Parietal Cortex

In Experiment 1, we localized tool-preferring regions in the dorsal and ventral streams. Participants viewed broad-band images of tools and animals arranged in category-homogenous miniblocks of 16 sec (32 stimuli, each presented for 500 msec; see Figure 1 for examples of the stimuli). Replicating previous studies (e.g., Mahon et al., 2007; Noppeney et al., 2006; Chao & Martin, 2000), viewing images of tools (compared with viewing animals) elicited differential activation in three left hemisphere regions—the left parietal cortex, the left middle temporal gyrus, and the left fusiform gyrus (false discovery rate [FDR], $q < .05$). Figure 2A shows a detail of the left parietal activation for tools compared with animals. This result demonstrates that the current set of materials generates the same topography of tool-preferring voxels as previous work.

In Experiment 2, we tested whether the left parietal tool-preferring region could be parcellated according to whether the tool preferences were carried by the LSF or the HSF information in the images. Tool preferences in parietal cortex were determined separately for HSF and LSF images, by contrasting HSF tools against HSF animals and, separately, LSF tools against LSF animals. The results (Figure 2B) indicate that tool preferences for HSF images are biased toward the inferior aspect of parietal tool-preferring cortex, whereas tool preferences for LSF images are biased toward the superior aspect of the left parietal tool-preferring cortex. Importantly, the contrast maps showing tool preferences in parietal cortex for HSF and LSF stimuli are independent; thus, there is no reason, in principle, why the two category contrasts could not lead to entirely overlapping populations of voxels (see also Figure 3 for overlap of the contrast maps from Experiments 1 and 2).

The finding that there is an inferior-to-superior organization within left parietal tool-preferring voxels according to the spatial frequency content of the images can be directly tied to what is known about the behavioral impairments that attend selective lesions to inferior or superior parietal regions. Optic ataxia, an impairment for reaching and/or grasping objects, is classically associated with lesions to posterior and superior parietal structures (Pisella et al., 2006; Goodale & Milner, 1992). Importantly, optic ataxia is not necessarily associated with difficulties for manipulating objects according to their function (once patients are able to prehend the objects). In contrast, an impairment for manipulating objects correctly according to their function, termed apraxia of object use, is classically associated with lesions to the left inferior parietal lobule (Johnson-Frey, 2004; Rushworth, Nixon, Renowden, Wade, & Passingham, 1997; Rothi, Ochipa, & Heilman, 1991). Furthermore, patients with apraxia of object use may be able to reach for and grasp objects normally (i.e., apraxia without optic ataxia).

The system that supports complex object-associated manipulations must be informed about the identity of the object, as object manipulations are specific to the identity and function of the object. This reasoning is in line with the pattern of findings that we have obtained: Object representations in inferior parietal regions are contingent on analysis of the visual input by ventral structures. A key expectation of this view is that there will be privileged functional connectivity between inferior parietal HSF tool-preferring voxels and ventral stream structures that also exhibit tool preferences. We tested this expectation in a series of time-course-based functional connectivity analyses.

ROI-based Analysis of Functional Connectivity between Parietal and Temporal Cortex

Several complementary analyses were carried out to test a key prediction made by the hypothesis that object representations in left inferior parietal regions are contingent on analysis of the visual input by ventral stream structures. In the first analysis, we localized the

left medial fusiform gyrus within the ventral stream, which is known to be a tool-preferring region, with the data from Experiment 1 (broadband stimuli; tools > animals; FDR, $q < .05$). The resulting fusiform ROI is depicted in Figure 4A and replicates previous observations using similar stimuli (e.g., Mahon et al., 2007; Noppeney et al., 2006; Chao, Haxby, & Martin, 1999). We then extracted the time series using data from Experiment 2 from (i) the left medial fusiform ROI (Figure 4A), (ii) the inferior HSF tool-preferring parietal region (Figure 2B, purple ROI), and the (iii) the superior LSF tool-preferring parietal region (Figure 3B, green ROI). Pearson correlation coefficients were used as measures of functional connectivity between each parietal region and the ventral stream ROI (after regression of noise confounds; see Methods above). There was greater functional connectivity between the left medial fusiform gyrus and the left inferior parietal ROI than between the left medial fusiform and the left superior parietal ROI ($t = 2.98$, $p < .02$, paired, two-tailed; see Figure 4B). This analysis is conservative because a different group of participants was used to define the ventral tool-preferring ROI.

We also repeated the analysis, defining the ventral tool-preferring ROI within Experiment 2, by collapsing across the factor spatial frequency and identifying voxels that responded more strongly to tool stimuli than animal stimuli (contrast: $\text{tools}_{(\text{HSF + LSF})} > \text{animals}_{(\text{HSF + LSF})}$; $p < .005$, corrected). The results of the connectivity analyses remained the same, indicating significantly greater connectivity between the inferior parietal HSF tool-preferring ROI and the ventral stream than between the superior parietal LSF tool-preferring ROI and the ventral stream ($t = 2.49$, $p < .03$).

To gain a deeper understanding of how connectivity to the two parietal ROIs was distributed across the population of voxels within the left medial fusiform gyrus, voxelwise histograms of connectivity were plotted. As shown in Figure 4C, there is a shift in the distributions of connectivity strength within the left medial fusiform voxels: More voxels express stronger connectivity to the left inferior HSF tool-preferring ROI than to the left superior LSF tool-preferring ROI. This difference was significant ($p < .001$), and the shift in the distributions was obtained regardless of whether the left fusiform was defined with the data from Experiment 1 (Figure 2B) or Experiment 2 (figure not shown; $p < .001$).

Whole-brain Analysis of Functional Connectivity

In a second set of functional connectivity analyses, the superior and inferior parietal ROIs were used as seeds in whole-brain analyses of connectivity. At the same threshold ($q < .05$, FDR corrected), the left medial fusiform gyrus was identified by the analysis in which the inferior parietal HSF tool-preferring ROI was used as a seed but not when the left LSF tool-preferring parietal ROI was used (Figure 5). This can be seen in the detailed depiction of the ventral stream (Figure 5A) in which voxels expressing connectivity to the left inferior parietal ROI are largely contained within the functionally defined left medial fusiform gyrus. Again, this correspondence was obtained both when the left medial fusiform ROI was defined with Experiment 1 and Experiment 2 (see Figure 5). In contrast, and constituting an important internal control, both parietal seeds identified the left middle temporal gyrus (lateral views, Figure 5).

Finally, we sought to test whether the spatial distribution of connectivity with inferior parietal regions matched the distribution of tool preferences in the ventral stream. To that end, a lateral-to-medial analysis was carried out over a region of the ventral stream that straddled both medial and lateral areas. This analysis takes a swath of volume space and "slices" it into 3-mm-thick "leaves," with each "leaf" in a plane defined by Talairach z (superior–inferior) and y (anterior–posterior) coordinates (for precedent, see Mahon, Anzellotti, Schwarzbach, Zampini, & Caramazza, 2009; see also Connolly et al., 2012). The statistic of interest (e.g., contrast- weighted t values) is then averaged within the "leaf" (i.e.,

along the anterior–posterior and inferior–superior dimensions) and plotted by lateral-to-medial location (Talairach *x* dimension). Two such lateral-to-medial analyses were carried out. The first was computed over the contrast-weighted *t* values for the contrast of tool $_{(HSF + LSF)}$ > animals$_{(HSF + LSF)}$ in Experiment 2. Replicating previous lateral-to-medial analyses of contrast-weighted statistics (Connolly et al., 2012; Mahon et al., 2009), tool preferences increase as the slices move more medial (blue line, Figure 6). The same lateral-to-medial analysis was then carried out over an index that represents the degree to which connectivity in the fusiform is differentially expressed to the inferior parietal ROI compared with the superior parietal ROI (IP = inferior parietal, SP = superior parietal: [connectivity with IP − connectivity with SP]/[connectivity with IP + connectivity SP]; see black line, Figure 6). The lateral-to-medial analysis of connectivity almost perfectly tracks the lateral-to-medial analysis of the contrast-weighted *t* value. Specifically, as the position within the fusiform gyrus becomes more medial, tools lead to higher BOLD contrast than animals, and there is also differential connectivity to inferior parietal cortex compared with superior parietal regions. This high level of correspondence within the ventral stream between connectivity to parietal cortex and tool preferences was observed regardless of whether the contrast-weighted *t* map of tool preferences was derived from Experiment 1 (R^2 = .93, p < .01; data not shown) or Experiment 2 (R^2 = .99, p < .001; as shown in Figure 6).

DISCUSSION

Models of conceptual representation in the human brain have been strongly influenced by the empirical fact that manipulable object stimuli, compared to a range of baselines, elicit differential BOLD contrast in regions of parietal cortex known to be involved in object prehension and use. Two theoretical inferences have been derived from that observation. The first is that increased BOLD contrast in parietal cortex reflects the automatic extraction of information about the way in which objects are typically manipulated by a dorsal visual route that is independent of the ventral stream. The second inference is that retrieval and simulation of the motor information involved in manipulating tools is a critical step in retrieving a tool concept from the visual presentation of a manipulable object. The findings that we have reported indicate that both assumptions need revision. The fact that tool preferences are observed in parietal cortex for stimuli that contain only HSF information indicates that at least some of the tool preferences in parietal cortex are contingent on analysis of the visual input by ventral stream structures. This conclusion is at odds with the hypothesis that recognition of manipulable objects is contingent on simulation of the motor movements associated with their use (for an overview, see Kiefer & Pulvermüller, 2012). This is because, if the motor simulation occurs only after the stimulus has been processed by ventral visual stream structures, then the stimulus has already gone through the classic channels of visual object identification. This conclusion converges with observations from brain-damaged patients showing that damage to the left inferior parietal lobule can lead to an impairment for manipulating objects, while sparing the ability to recognize objects (for reviews, see Mahon & Caramazza, 2008; Johnson-Frey, 2004; Rothi et al., 1991). This conclusion also converges with prior arguments that the inferior parietal lobule and the functions it subserves should not be considered to be part of the dorsal visual pathway (Pisella et al., 2006; Rizzolatti & Matelli, 2003; Milner & Goodale, 1995; for a parallel discussion of the right inferior parietal lobule, see Singh-Curry & Husain, 2009).

It was also observed that superior parietal regions show tool preferences for images that contain only LSF information. Neuropsychological data indicate that damage to superior parietal regions can lead to visuomotor impairments for reaching and grasping objects. Thus, within the context of the embodied cognition hypothesis, it might be argued that the critical motor simulation is not of complex object manipulation (inferior parietal) but of the handshape configuration(s) that are implicated by object grasps. That direction for

reconfiguring the proposal faces several difficulties. First, hand configurations appropriate for grasping objects will be shared by similarly shaped objects; thus, it is not at all clear that knowing the hand configuration appropriate for grasping an object could provide any individuating information that could contribute to distinguishing a stimulus from perceptual neighbors. Second, one of the original phenomena that motivated the proposal of a separation between ventral and dorsal visual streams was the dissociation between object prehension and object recognition (optic ataxia vs. visual form agnosia). Thus, we know that patients with lesions to posterior–superior parietal cortex can be impaired for object prehension but spared for visual recognition (for a discussion, see Goodale & Milner, 1992; for a relevant conceptual analysis, see Wu, 2008).

The hypothesis that the retrieval of complex object-associated manipulation knowledge is contingent on analysis of the visual input by the ventral visual pathway is not incompatible with the hypothesis that the retrieval of object use knowledge is automatic. However, if the activation of object use information is in fact automatic and, yet, not necessary for recognition, then a cascading model of the dynamics of activation flow between concepts and object use information is strongly suggested (for discussion of dynamics as it relates to the embodied cognition hypothesis, see Mahon & Caramazza, 2008). Independent of these considerations about the dynamical principles that characterize the concept–motor interface, our findings show that the automatic activation of parietal cortex when viewing tools does not monolithically represent processing of the visual input by the dorsal visual pathway. Differential BOLD responses to manipulable objects in parietal cortex reflect comingling of information extracted by the ventral stream with motor-based information represented in parietal regions as well as the computation of reach-and-grasp information by the (classically understood) dorsal visual pathway.

One objection that may be raised is that the “classic” construal of the function of the dorsal stream is itself insufficient. Recently, the classic view of the division of labor between the dorsal and ventral visual streams has been questioned in light of evidence that object representations in posterior parietal regions exhibit response characteristics that generalize across image transformations (Konen & Kastner, 2008). Konen and Kastner’s findings indicate that object representations in parietal cortex are abstracted away from the particular image characteristics of the stimuli, a property that may not be expected by the classic understanding of the dorsal stream. Those data, in the context of our current findings, outline a new framework for exploring whether there are mutual dependencies between the representations in the dorsal and ventral visual systems and, if so, over what types of information those dependencies are expressed. For instance, one open issue is whether regions of parietal cortex that show invariance in BOLD responses across image transformations derive their input entirely from a dorsal analysis of the visual input or are also (in part) contingent on analysis of the visual input by ventral stream structures.

Another, and related, question that may be raised is whether the tool preferences for HSF stimuli in the left inferior parietal lobule are supported by the limited parvocellular channels that do putatively project to parietal cortex. In other words, perhaps, parvocellular analysis of the visual input bypasses the ventral stream and subserves the tool preferences for HSF stimuli in the left inferior parietal lobule. One argument against this interpretation is the pattern of functional connectivity that we have reported between the left inferior parietal lobule and the left medial fusiform gyrus. Those functional connectivity results increase the likelihood that the effects observed in the left inferior parietal lobule are in fact tied to processing in the ventral stream. Nevertheless, the broader point is that the functions of the classically understood dorsal visual pathway are functions largely attributable to magnocellular analysis (e.g., fast conductance, luminance based, sensitive to fast motion, etc.; Merigan & Maunsell, 1993; Goodale & Milner, 1992). Thus, even if the tool effects in

the left inferior parietal lobule were driven by the small proportion of inputs to posterior parietal cortex that are parvocellular, then the inference would still be sanctioned that the representations in the left inferior parietal lobule are not part of the classically understood dorsal stream. This conclusion is consistent with the initial suggestions made by Goodale and Milner (1992).

The stronger conclusion, and which we favor, is that the tool preferences in the left inferior parietal lobule are in fact contingent on analysis of the visual input by the ventral object processing stream. A critical test of this stronger conclusion would be provided by studying the distribution of tool preferences in parietal cortex in patients with lesions to the ventral stream. The framework that we have outlined predicts that patients with ventral stream lesions affecting the visual and semantic analysis of manipulable object stimuli will continue to show normal tool responses in posterior and superior parietal regions but will have attenuated or even abolished responses in the left inferior parietal lobule.

In summary, and together with prior neuropsychological research, our findings suggest an alternative to the embodied cognition hypothesis of tool recognition: The activation of (at least some) motor-relevant information in parietal cortex is contingent on processing within the ventral stream. On this view, motor-relevant information about object use is not a necessary intermediary step in object recognition (Chatterjee, 2010; Mahon & Caramazza, 2008; Machery, 2007). An interesting issue for future research is whether previously described white matter connectivity between the temporal and parietal lobules (Rushworth, Behrens, & Johansen-Berg, 2006; Zhong & Rockland, 2003) is the basis for the integration of information about object identity with information about object-associated manipulations.

Acknowledgments

This research was supported by NIH Grant R21 NS076176 from NINDS to B. Z. M. J. A. was supported by Fundação para a Ciência e a Tecnologia fellowship SFRH/BPD/70970/2010 and by EU-FP7/2007-2013, under PCOFUND-GA-2009-246542. This research was supported in part by Norman and Arlene Leenhouts. The authors are grateful to Jessica Cantlon, Greg DeAngelis, and Bill Merigan for discussion.

REFERENCES

Barsalou LW. Perceptual symbol systems. Behavioral and Brain Sciences. 1999; 22:577–609. discussion 610-560. [PubMed: 11301525]

Brainard DH. The Psychophysics Toolbox. Spatial Vision. 1997; 10:433–436. [PubMed: 9176952]

Buccino G, Riggio L, Melli G, Binkofski F, Gallese V, Rizzolatti G. Listening to action related sentences modulates the activity of the motor system: A combined TMS and behavioral study. Cognitive Brain Research. 2005; 24:355–363. [PubMed: 16099349]

Chao LL, Haxby JV, Martin A. Attribute-based neural substrates in temporal cortex for perceiving and knowing about objects. Nature Neuroscience. 1999; 2:913–919.

Chao LL, Martin A. Representation of manipulable man-made objects in the dorsal stream. Neuroimage. 2000; 12:478–484. [PubMed: 10988041]

Chatterjee A. Disembodying cognition. Language and Cognition. 2010; 2:79–116. [PubMed: 20802833]

Connolly AC, Guntupalli JS, Gors J, Hanke M, Halchenko YO, Wu Y-C, et al. The representation of biological classes in the human brain. The Journal of Neuroscience. 2012; 32:2608–2618. [PubMed: 22357845]

Derrington AM, Lennie P. Spatial and temporal contrast sensitivities of neurones in lateral geniculate nucleus of macaque. Journal of Physiology (London). 1984; 357:219–240. [PubMed: 6512690]

Felleman DJ, Van Essen DC. Distributed hierarchical processing in primate visual cortex. Cerebral Cortex. 1991; 1:1–47. [PubMed: 1822724]

Ferrera VP, Nealey TA, Maunsell JHR. Mixed parvocellular and magnocellular geniculate signals in visual area V4. Nature. 1992; 358:756–758. [PubMed: 1508271]

Gallese V, Lakoff G. The brain's concepts: The role of the sensory-motor system in conceptual knowledge. Cognitive Neuropsychology. 2005; 22:455–479. [PubMed: 21038261]

Goodale MA, Milner AD. Separate visual pathways for perception and action. Trends in Neurosciences. 1992; 15:20–25. [PubMed: 1374953]

Johnson-Frey SH. The neural bases of complex tool use in humans. Trends in Cognitive Sciences. 2004; 8:71–78. [PubMed: 15588811]

Kiefer M, Pulvermüller F. Conceptual representations in mind and brain: Theoretical developments, current evidence and future directions. Cortex. 2012; 48:805–825. [PubMed: 21621764]

Konen CS, Kastner S. Two hierarchically organized neural systems for object information in human visual cortex. Nature Neuroscience. 2008; 11:224–231.

Livingstone M, Hubel D. Segregation of form, color, movement, and depth: Anatomy, physiology, and perception. Science. 1988; 240:740–749. [PubMed: 3283936]

Machery E. Concept empiricism: A methodological critique. Cognition. 2007; 104:19–46. [PubMed: 16814274]

Mahon BZ, Anzellotti S, Schwarzbach J, Zampini M, Caramazza A. Category-specific organization in the human brain does not require visual experience. Neuron. 2009; 63:397–405. [PubMed: 19679078]

Mahon BZ, Caramazza A. A critical look at the embodied cognition hypothesis and a new proposal for grounding conceptual content. Journal of Physiology (Paris). 2008; 102:59–70.

Mahon BZ, Milleville SC, Negri GA, Rumiati RI, Caramazza A, Martin A. Action-related properties shape object representations in the ventral stream. Neuron. 2007; 55:507–520. [PubMed: 17678861]

Martin, A.; Ungerleider, LG.; Haxby, JV. Category specificity and the brain: The sensory/motor model of semantic representations of objects. In: Gazzaniga, MS., editor. Higher cognitive functions: The new cognitive neurosciences. Cambridge, MA: MIT Press; 2000. p. 1023-1036.

Maunsell JHR, Nealey TA, DePriest DD. Magnocellular and parvocellular contributions to responses in the middle temporal visual area (MT) of the macaque monkey. Journal of Neuroscience. 1990; 10:3323–3334. [PubMed: 2213142]

Merigan WH, Maunsell JH. How parallel are the primate visual pathways? Annual Review of Neuroscience. 1993; 16:369–402.

Milner, AD.; Goodale, MA. The visual brain in action. Oxford, UK: Oxford University Press; 1995.

Noppeney U, Price CJ, Penny WD, Friston KJ. Two distinct neural mechanisms for category-selective responses. Cerebral Cortex. 2006; 16:437–445. [PubMed: 15944370]

Pelli DG. The VideoToolbox software for visual psychophysics: Transforming numbers into movies. Spatial Vision. 1997; 10:437–442. [PubMed: 9176953]

Pisella L, Binkofski F, Lasek K, Toni I, Rossetti Y. No double-dissociation between optic *ataxia* and visual agnosia: Multiple sub-streams for multiple visuo-manual integrations. Neuropsychologia. 2006; 44:2734–2748. [PubMed: 16753188]

Rizzolatti G, Matelli M. Two different streams form the dorsal visual system: Anatomy and functions. Experimental Brain Research. 2003; 153:146–157.

Rothi LJG, Ochipa C, Heilman KM. A cognitive neuropsychological model of limb praxis. Cognitive Neuropsychology. 1991; 8:443–458.

Rushworth MF, Behrens TE, Johansen-Berg H. Connection patterns distinguish 3 regions of human parietal cortex. Cerebral Cortex. 2006; 16:1418–1430. [PubMed: 16306320]

Rushworth MF, Nixon PD, Renowden S, Wade DT, Passingham RE. The left parietal cortex and motor attention. Neuropsychologia. 1997; 35:1261–1273. [PubMed: 9364496]

Schwarzbach J. A simple framework (ASF) for behavioral and neuroimaging experiments based on the psychophysics toolbox for MATLAB. Behavior Research Methods. 2011; 43:1194–1201. [PubMed: 21614662]

Singh-Curry V, Husain M. The functional role of the inferior parietal lobe in the dorsal and ventral stream dichotomy. Neuropsychologia. 2009; 47:1434–1448. [PubMed: 19138694]

Talairach, J.; Tournoux, P. Co-planar stereotaxic atlas of the human brain. New York: Thieme; 1988.

Tootell RB, Silverman MS, Hamilton SL, Switkes E, De Valois RL. Functional anatomy of macaque striate cortex. V. Spatial frequency. Journal of Neuroscience. 1988; 8:1610–1624. [PubMed: 3367213]

Ungerleider, LG.; Mishkin, M. Two cortical visual systems. In: Goodale, MA.; Mansfield, RJW., editors. Analysis of visual behavior. Cambridge, MA: The MIT Press; 1982. p. 549-586.

Wu WC. Visual attention, conceptual content, and doing it right. Mind. 2008; 117:1003–1033.

Zhong Y-M, Rockland KS. Inferior parietal lobule projections to anterior inferiortemporal cortex (area TE) in macaque monkey. Cerebral Cortex. 2003; 13:527–540. [PubMed: 12679299]

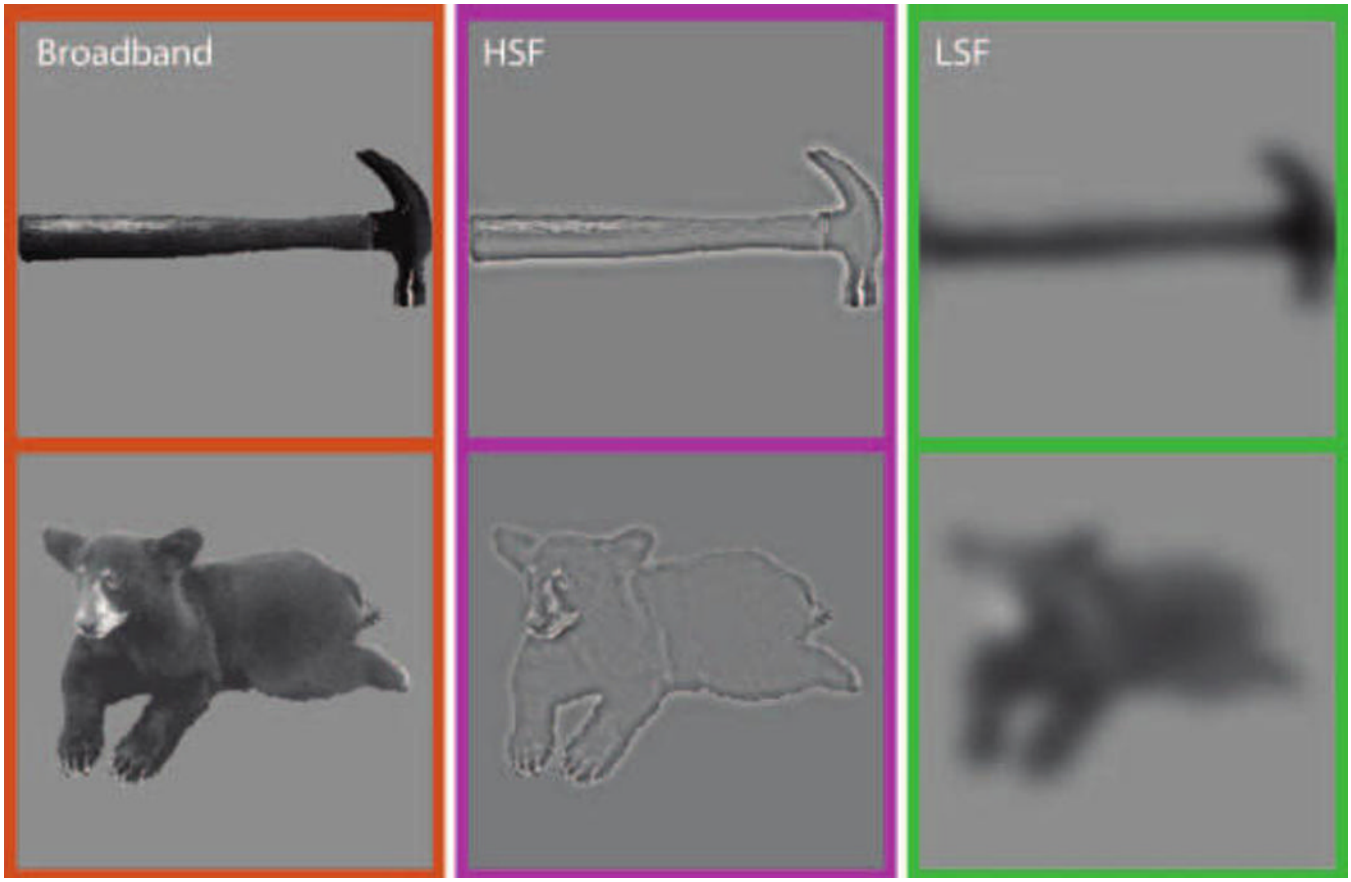

Figure 1.
Examples of stimuli used in Experiments 1 and 2. The same set of grayscale tools and animals were used across both experiments. The images were broadband in Experiment 1 and filtered to contain only HSF or LSF information in Experiment 2.

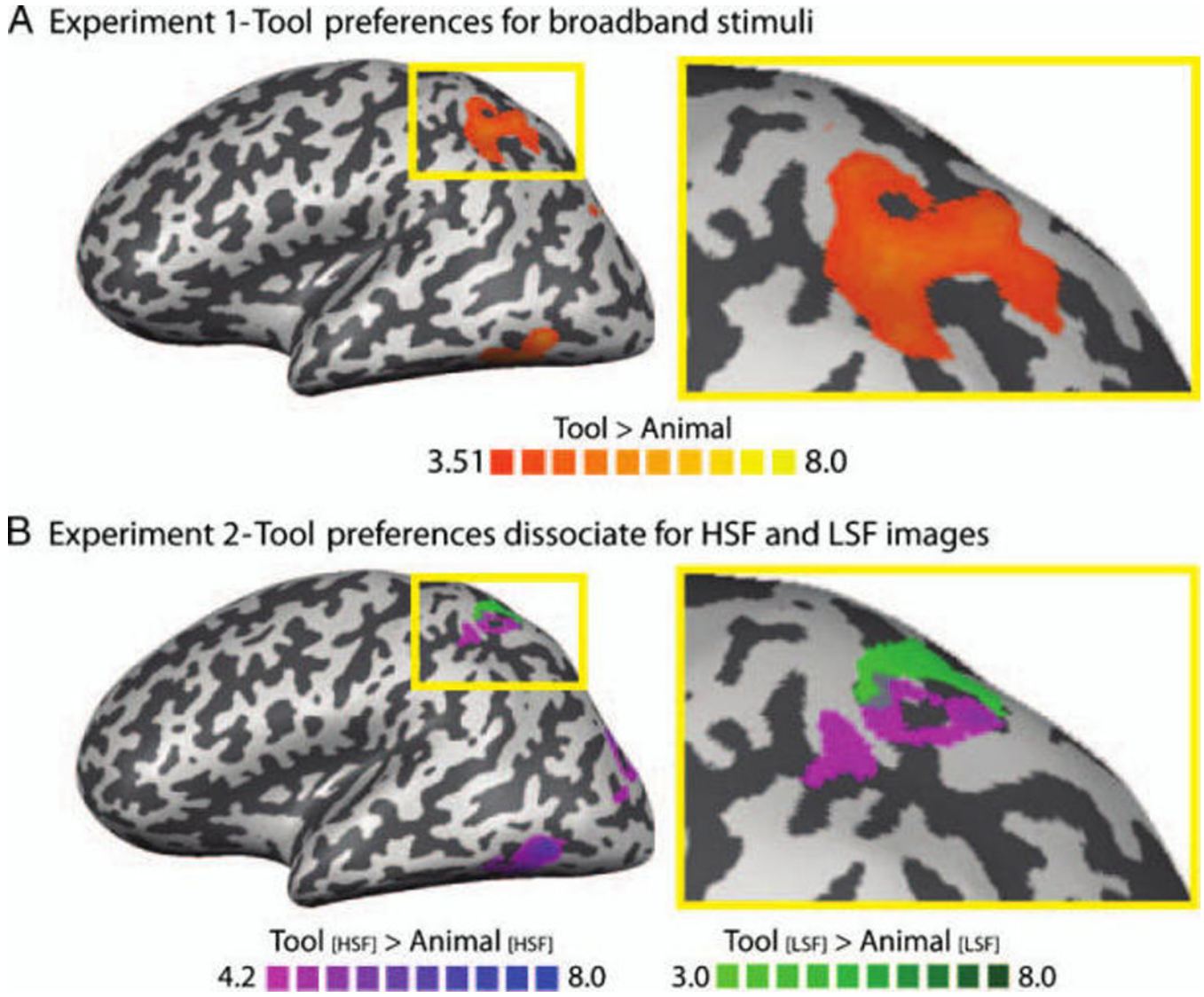

Figure 2.

Tool-preferring regions in the left parietal cortex dissociate according to the spatial frequency content of the images. (A) Detail of left parietal tool-preferring voxels in Experiment 1 (FDR, $q < .05$) obtained using standard (broadband) grayscale images. (B) Detail of the left parietal regions defined by the contrasts of $tools_{HSF} > animals_{HSF}$ (purple) and $tools_{LSF} > animals_{LSF}$ (green; both maps: $p < .05$, corrected). These contrasts, which are independent and so have no bias against showing overlap, indicate a dissociation along the inferior-to-superior dimension in whether the tool preference is differentially carried by HSF or LSF information in the images.

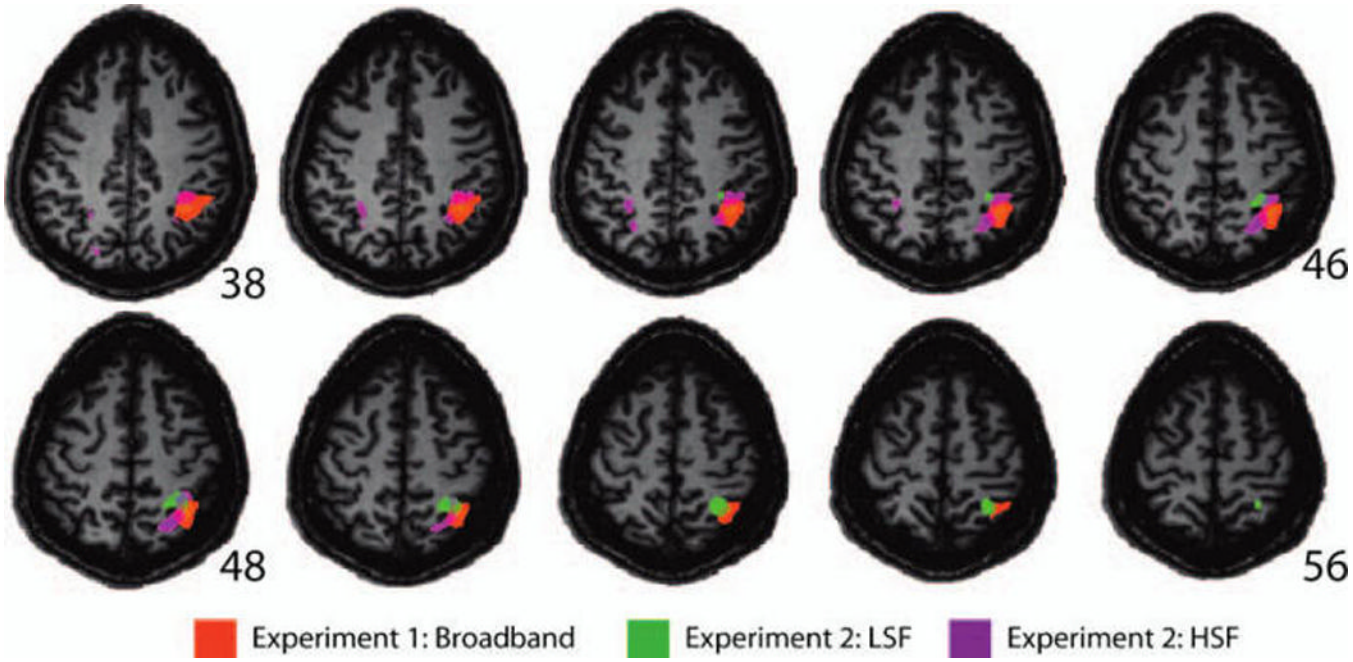

Figure 3.

Overlap of contrast maps for Experiments 1 and 2 in the left parietal cortex. Plotted on the orange color scale is the contrast of tool > animal (FDR, $q < .05$) from Experiment 1. Plotted on the purple color scale is the contrast $tool_{HSF} > animal_{HSF}$, and plotted on the green color scale is the contrast $tool_{LSF} > animal_{LSF}$, both from Experiment 2 ($p < .05$, corrected). Within the left parietal cortex, more inferior aspects show tool preferences for HSF images, whereas more superior regions exhibit tool preferences for LSF images.

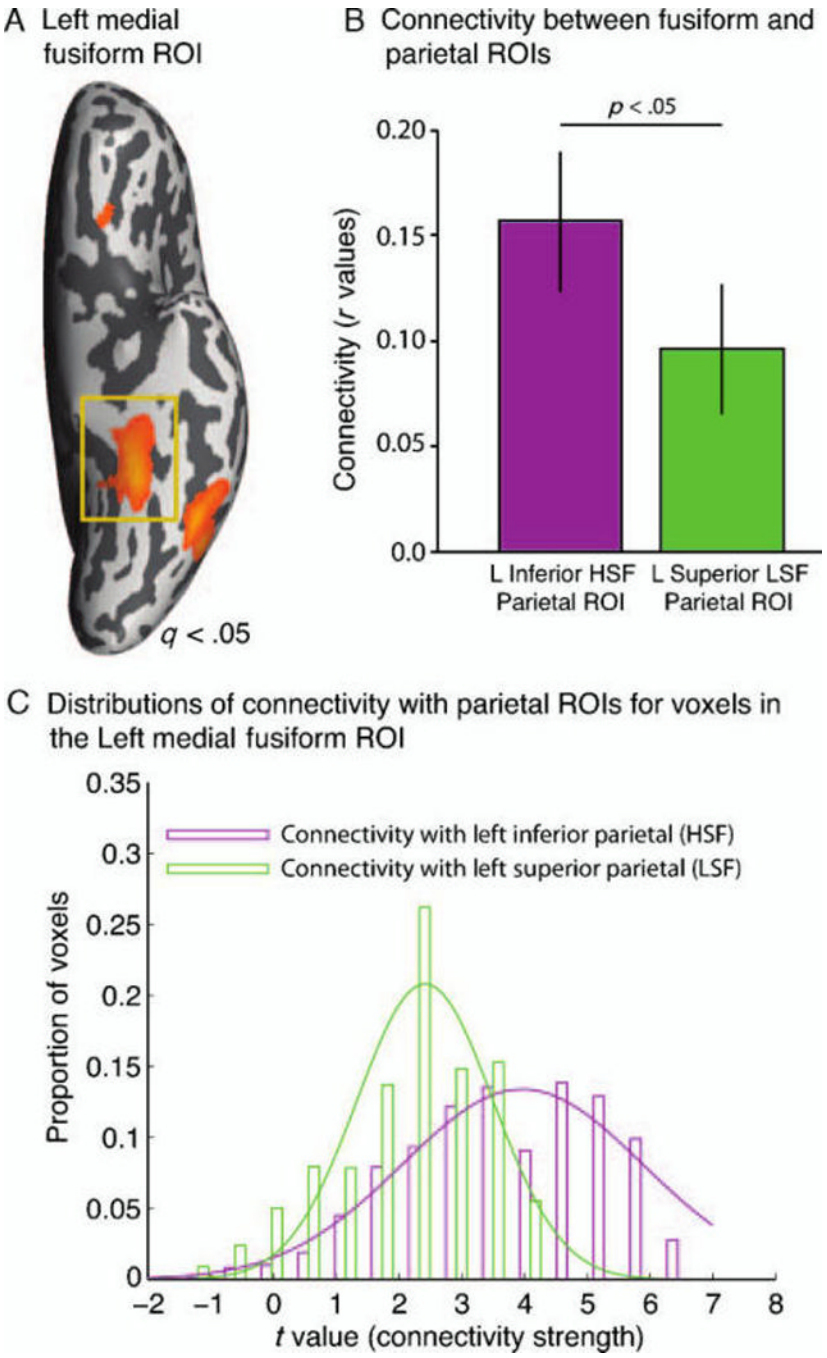

Figure 4.

The inferior HSF tool-preferring parietal region exhibits privileged connectivity with the left medial fusiform gyrus. (A) The medial fusiform ROI from Experiment 1 is shown, defined by the contrast tools > animals (FDR, $q < .05$). (B) Time-course-based functional connectivity analyses were conducted using time-series data from the left medial fusiform ROI (A) and the inferior and superior parietal ROIs (Figure 2B). There was significantly greater connectivity between the left medial fusiform ROI and the inferior parietal ROI compared with the superior parietal ROI. Error bars reflect *SEM*s across participants. (C) Voxelwise connectivity values (*t* values for the group-level analysis) of connectivity with the two parietal ROIs were extracted for each voxel within the left medial fusiform gyrus

and plotted as histograms. The results indicate a shift in the distributions, with stronger connectivity between the medial fusiform voxels and the inferior parietal ROI compared with the superior parietal ROI. L = left.

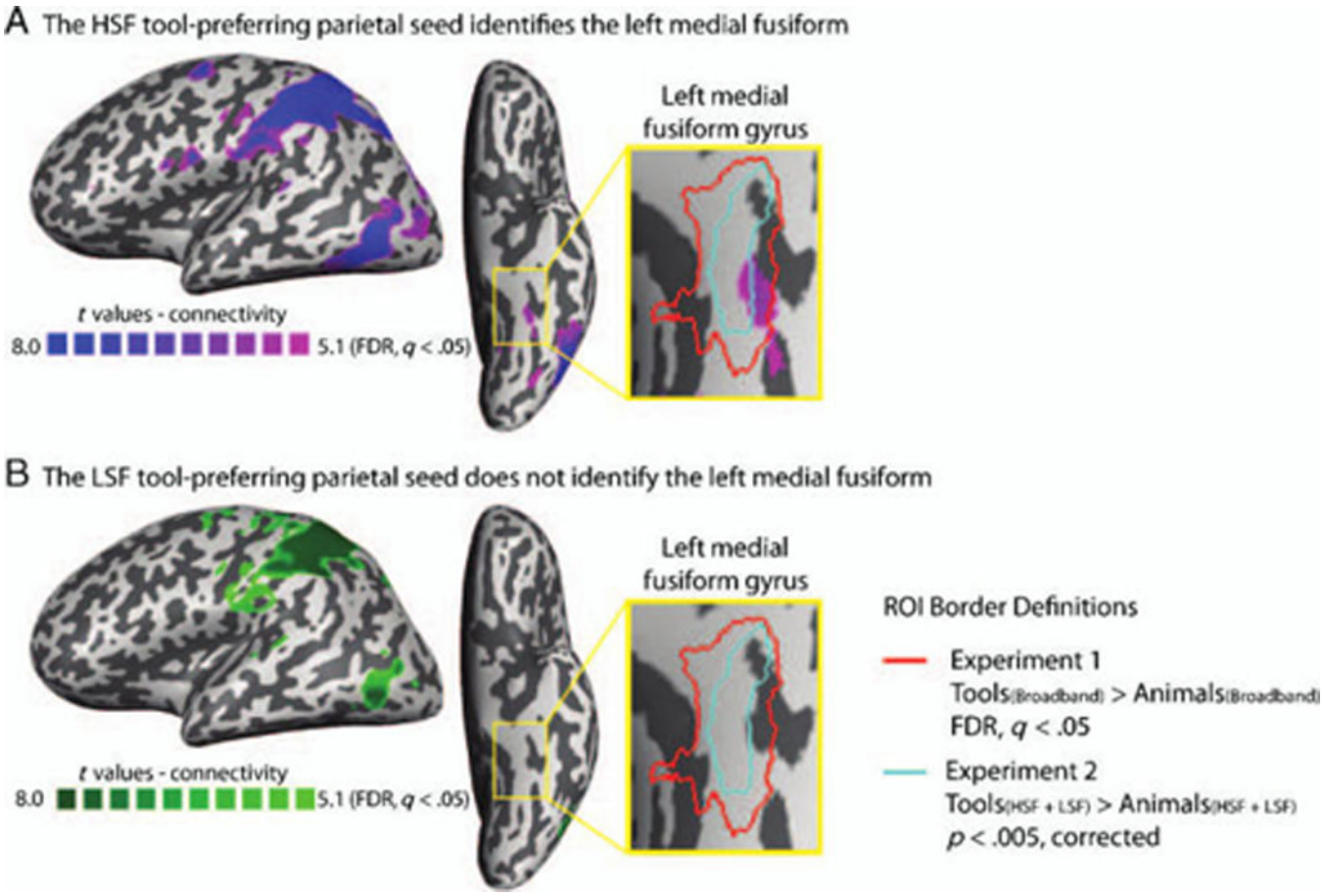

Figure 5.

Whole-brain functional connectivity maps were computed using the inferior and superior parietal ROIs (from Figure 2). Group-level statistics were computed as one-sample *t* tests (voxelwise) over participants' connectivity values. (A) Group-level *t* map for connectivity with the left inferior HSF tool-preferring parietal ROI. The detail shows that the connectivity analysis identifies voxels in the left medial fusiform gyrus, as functionally defined with either Experiment 1 (red border) or Experiment 2 (blue border). (B) Group-level *t* map for connectivity with the left superior LSF tool-preferring parietal ROI. As shown in the detailed image, connectivity with the superior parietal ROI is absent within the independently defined medial fusiform ROIs. All *t* maps were thresholded at FDR, $q < .05$.

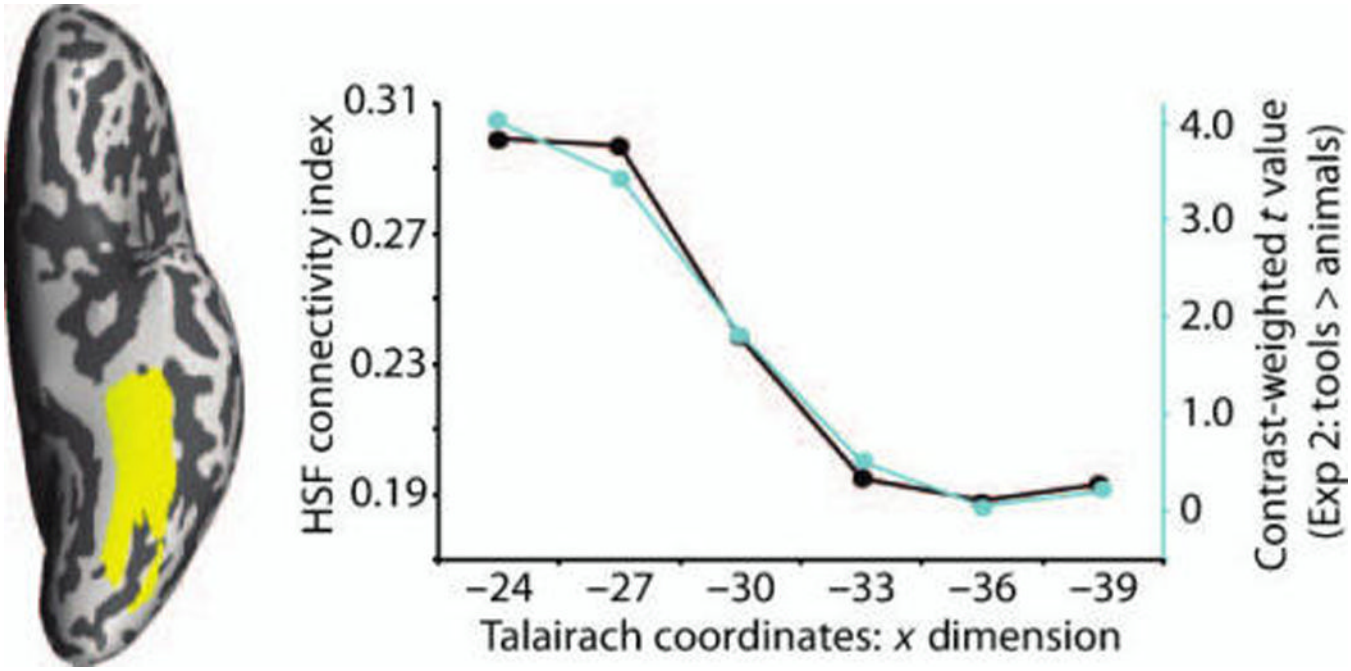

Figure 6.

Lateral-to-medial analysis of ventral stream tool preferences and connectivity with parietal cortex. Two independent lateral-to-medial analyses were computed by averaging the relevant statistic along the Talairach *z* (inferior–superior) and *y* (anterior–posterior) axes for each Talairach *x* dimension value (binned at 3 mm). In one analysis, the lateral-to-medial index for the contrast-weighted *t* value measuring tool preferences (tools > animals) was computed (light blue line). In a second lateral-to-medial analysis, differential connectivity to the left inferior parietal ROI was determined: (connectivity with inferior parietal ROI − connectivity with superior parietal ROI)/(connectivity with inferior parietal ROI + connectivity with superior parietal ROI). The results of the two independent analyses demonstrate correspondence along the lateral-to-medial dimension. Exp = experiment.